EPJ Web of Conferences **33**, 02001 (2012)
DOI: 10.1051/epjconf/20123302001

TBCs for Gas Turbines under Thermomechanical Loadings: Failure Behaviour and Life Prediction

T. Beck[1,a], O. Trunova[1], R. Herzog[2], and L. Singheiser[1]

[1]Forschungszentrum Juelich GmbH, Institute of Energy and Climate Research, 52425 Juelich, Germany
[2]MAN Turbo AG, Oberhausen, Germany

Abstract. The present contribution gives an overview about recent research on a thermal barrier coating (TBC) system consisted of (i) an intermetallic MCrAlY-alloy Bondcoat (BC) applied by vacuum plasma spraying (VPS) and (ii) an Yttria Stabilised Zirconia (YSZ) top coat air plasma sprayed (APS) at Forschungszentrum Juelich, Institute of Energy and Climate Research (IEK-1). The influence of high temperature dwell time, maximum and minimum temperature on crack growth kinetics during thermal cycling of such plasma sprayed TBCs is investigated using infrared pulse thermography (IT), acoustic emission (AE) analysis and scanning electron microscopy. Thermocyclic life in terms of accumulated time at maximum temperature decreases with increasing high temperature dwell time and increases with increasing minimum temperature. AE analysis proves that crack growth mainly occurs during cooling at temperatures below the ductile-to-brittle transition temperature of the BC. Superimposed mechanical load cycles accelerate delamination crack growth and, in case of sufficiently high mechanical loadings, result in premature fatigue failure of the substrate. A life prediction model based on TGO growth kinetics and a fracture mechanics approach has been developed which accounts for the influence of maximum and minimum temperature as well as of high temperature dwell time with good accuracy in an extremely wide parameter range.

1 Introduction

Improving gas turbine power output and efficiency by increasing turbine inlet temperatures is possible by appropriate cooling concepts combined with thermal barrier coatings applied on turbine blades and vanes. Currently used thermal barrier coatings (TBCs) typically consist of a ceramic top coat and a metallic bond coat (BC) [1,2]. During cyclic operation the hot section components of gas turbines undergo complex thermal and mechanical loadings. As a result, thermomechanical fatigue (TMF) is one of the main lifetime limiting factors, especially for turbine blades and vanes.

The performance of the TBC under TMF loadings is related to the thermal and mechanical strains generated by temperature gradients and thermal mismatch as well as to the oxidation of BC. It is important to identify the parameters which affect the crack growth mechanism and thus the

[a] e-mail : t.beck@fz-juelich.de

lifetime of thermal barrier coatings [3,4]. However, studies on TMF behaviour of TBC systems reported in the literature are limited and differences in experimental procedure make the comparison of published results very difficult. Both, failure by TBC spallation of and fatigue failure of bond coat and base material have been reported [5,6], but systematic investigations on the type and details of failure are not available up to now.

The present paper addresses the effect of high temperature dwell time on the failure mode and lifetime of APS TBCs under thermal cycling and TMF loadings. Furthermore, the TBC life prediction model described in [7] has been improved and validated using experimental data obtained under thermal cycling with variation of the maximum and minimum temperature.

2 Experimental

The investigated TBC system consisted of the single crystal Ni-base superalloy CMSX-4 as substrate, a vacuum plasma-sprayed (VPS) NiCoCrAlY bond coat and an atmospherically plasma sprayed (APS) TBC of zirconia partially stabilized with about 8 wt.% yttria (YSZ). The bond coat thickness was ~150 µm and the TBC thickness ~300 µm.

Thermal cycling tests were carried out in an infrared furnace from Xerion GmbH with a power of 6 kW. The temperature was controlled using a pyrometer calibrated before with Pt/Pt-Rh-thermocouples. Cooling of the specimens was enhanced by compressed air flow directed to the specimen surface. Hollow cylindrical specimens with an internal diameter of 6.85 mm, an external diameter of 8.5 mm and a length of 25 mm were used.

For TMF tests hollow cylindrical specimens with 6.85 mm internal diameter and 10 mm external diameter over the gauge length of 20 mm were used. The experiments were conducted using a servohydraulic testing machine (Instron, model 8802) with a 100 kN static/50 kN dynamic load cell equipped with an 24 kW - infrared furnace from Xerion GmbH. Enhanced cooling was achieved by compressed air flow directed to the specimen surface. The temperature was controlled using 3 pyrometers along the gauge length, which were calibrated with Pt/Pt-Rh-thermocouples. The specimen deformation was monitored using a high temperature extensometer from MTS systems GmbH. Before the tests the samples were stained with iron oxide to improve the absorption of the IR radiation to the specimen surface.

The thermal cycles consisted of heating with a rate of 2°C/s followed by a dwell time at maximum temperature, cooling to minimum temperature with 2°C/s and 1 minute dwell time at minimum temperature. Details about in situ acoustic emission analysis during thermal cycling are given elsewhere [8].

The TMF tests were carried out according to the European Code-of-Practice for strain controlled TMF testing [9] with a mechanical strain range of 0.6% and a temperature range of 350°C-1050°C. The same cooling/heating rate of 2°K/s was used as for thermal cycling. Symmetrical out-of-phase (OOP) TMF and in-phase (IP) cycles with and without dwell time at maximal temperature were carried out.

The microstructural investigations were performed after metallographic preparation using optical microscopy (Leica – MEF4M) as well as scanning electron microscopy (LEO 1530 – ‘Gemini’).

3 Results and discussion

3.1 Experiments

3.1.1 Thermal cycling

A series of thermal cycling tests in the temperature range 60–1050°C with 2 hours high temperature dwell time was carried out to investigate damage evolution, microstructure changes and failure of APS TBCs, as reported and discussed in [10]. It was shown that during the first phase of

delamination crack growth the crack length is strongly correlated with the thickness of the thermally grown oxide (TGO) formed between BC and TBC during high temperature exposure. As soon as certain crack length, which depends on the BC/TBC interface roughness, is reached, accelerated crack growth driven by TGO growth and thermal mismatch stresses was observed. Fig. 1a shows the TBC microstructure after failure at 700 cycles: the delamination crack propagated partly through the TGO and partly through the TBC layer.

Increasing minimum cycle temperature from 60 °C to 350 °C and to 700°C led to an increase in TBC lifetime. Failure occurred after 1440 and 2250 cycles, corresponding to 2880 and 4500 hours exposure time at 1050 °C, respectively. Thus, the lifetime in latter case is, in terms of high temperature exposure time, the same as reported in [10] for isothermal tests at 1050°C. Furthermore, the longer exposure times resulted in thicker TGO compared to cycling in the temperature range 60–1050 °C. This led to a shift of the spallation crack path towards the TGO, as shown in Fig. 1b and c. Increasing the maximum cycle temperature from 1050°C to 1100°C resulted in decrease of TBC cyclic life. In Fig.1d the delamination failure after 437 cycles is represented.

In addition, thermal cycling experiments with 20 minutes high temperature dwell time in temperature ranges 60-1000°C, 60-1050°C and 60-1100°C proved that the number of cycles to failure decreases with increasing maximum cycle temperature. The delamination failure occurred after 2432, 1827 and 670 cycles, respectively. The lifetimes as a function of T_{min} and T_{max} for the high temperature dwell times of 2 hours and 20 minutes, respectively, are summarized in Fig 2a.

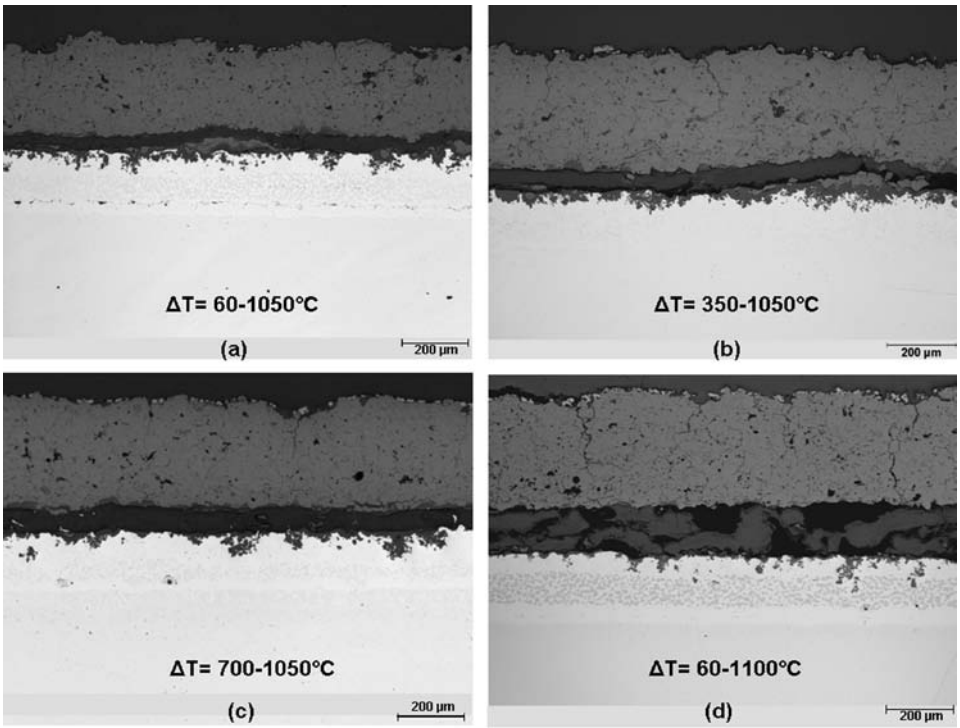

Fig. 1. Longitudinal sections after thermal cycling with 2 h high temperature dwell time: (a)-(c) variation of T_{min} and (d) variation of T_{max}

Acoustic emission analysis applied in situ during thermal cycling in temperature range 60-1050°C, as reported in [8], proved that damage occurred during cooling at temperatures below the ductile-to-brittle transition temperature of the BC due to an increase in thermally induced stresses at the TBC/BC interface. With decreasing temperature range of the thermal cycle (increase of minimum temperature) thermal stresses contribute less to TBC degradation compared to the

thermally activated damage processes, especially TGO growth. This is in good agreement with the increasing lifetimes observed with increasing T_{min}.

Furthermore, TBC lifetime in terms of number of cycles to failure decreases with increasing high temperature dwell time for thermal cycling in temperature range 60-1050°C, as reported in [10]. Additional thermal cycling experiments in temperature range 60-1100°C revealed a similar dependency, as shown in Fig.2b. These experimental results are used for improvement and validation of the life prediction model presented in section 3.2.

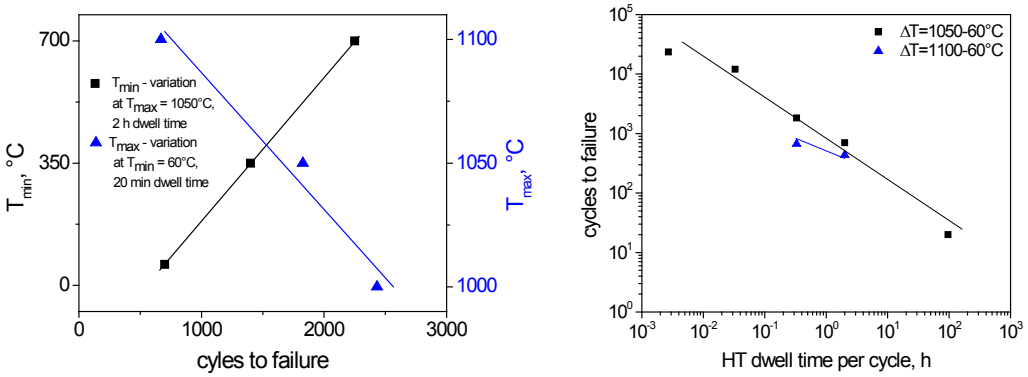

Fig. 2. TBC lifetimes under thermal cycling as a function of (a) T_{min} and T_{max} and (b) HT dwell time

3.1.2 Thermomechanical fatigue

Compared to thermal cycling, TMF loadings resulted in additional damage mechanisms. Depending on the TMF cycle parameters TBC failure occurred due to accelerated delamination crack growth at the TBC/BC interface or due to premature fatigue failure of the substrate. Detailed micrographs of the TBC/BC/base material interfaces are illustrated in Fig.3.

Both OOP and IP TMF with 2 hours high temperature dwell time resulted in spallation of the TBC (Fig.3a and b). The delamination crack is located partly within the TGO and partly within the TBC. The number of cycles to failure was 619 and 531, respectively. Thus, lifetime decreased compared to thermal cycling in the same temperature range (see Fig. 2a).

In contrast, under TMF without high temperature dwell time typically fatigue damage and failure of the base material occurred (Fig.3c and d). Some delamination cracks propagating within the TBC close to the TBC/TGO interface were observed too, but they did not lead to spallation before fatigue failure. The number of cycles to failure is higher (1620 and 3600 cycles for OOP and IP TMF, respectively) than for tests with dwell time. In Fig. 4 the dependence of TMF lifetimes on the cycle parameters is shown.

Under OOP TMF the tensile stresses applied at low temperatures led to preferred crack initiation in the valley regions of the TGO/BC interface profile due to the as stress concentration at these locations. Fatigue cracks propagated perpendicular to the loading direction into the bond coat and stopped at the BC/substrate interface in case of TMF with dwell time or penetrated into the substrate for TMF test without dwell time (Fig.3a and c). Fatigue crack growth mechanisms in BC under OOP TMF with and without dwell time at high temperature are discussed in detail elsewhere [11].

Under IP TMF the tensile stresses at high temperatures resulted in creep of bond coat. Therefore, in contrast to OOP TMF no cracks were observed to form in the bond coat. Instead, fatigue crack initiation took place in the substrate material at pores as well as at the inner surface of the hollow specimen. In IP TMF tests without dwell time these cracks penetrated into the bond coat before spallation failure of the TBC, as shown in Fig. 3d.

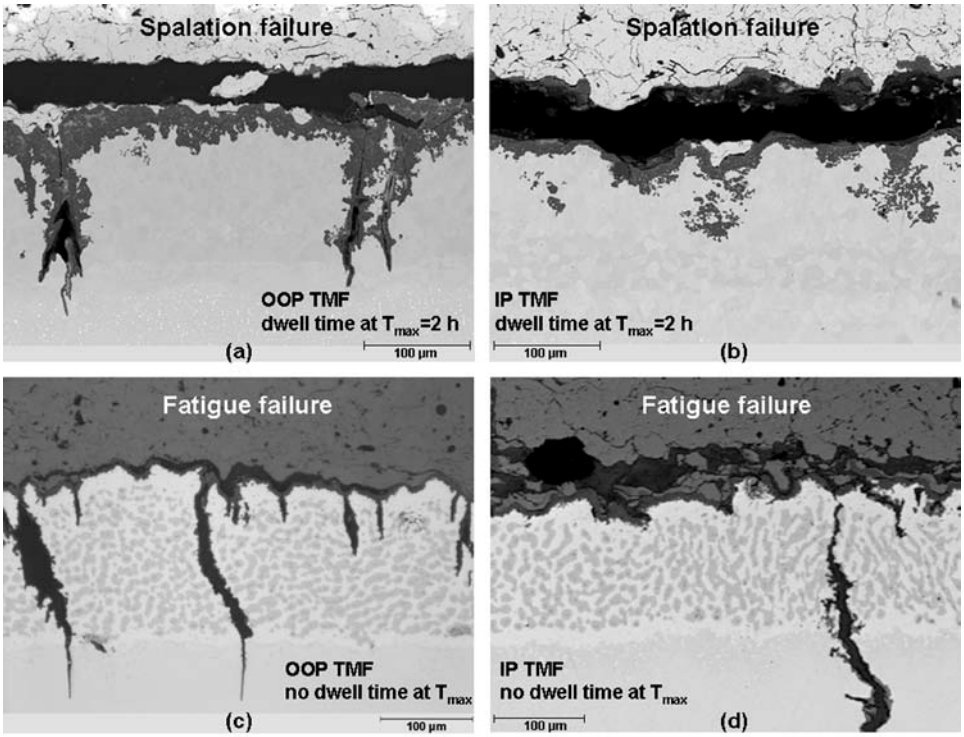

Fig. 3. Longitudinal sections after TMF experiments in the temperature range 350-1050°C with a mechanical strain range of 0.6%: with 2h HT dwell time (a) OOP, (b) IP and without HT dwell time (c) OOP, (d) IP.

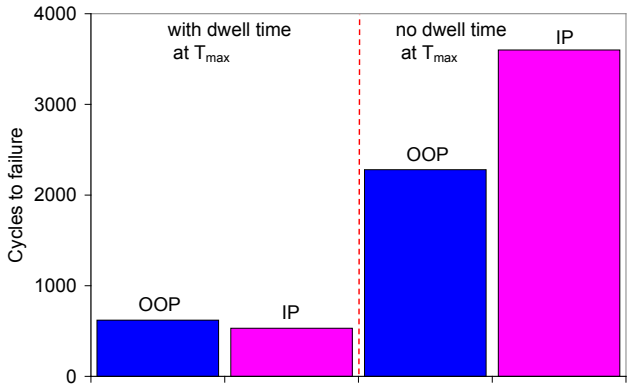

Fig. 4. Dependence of TBC lifetime on TMF cycle type and high temperature dwell time

3.2 Lifetime prediction for thermocyclic loading

3.2.1 Calculation of crack length

It is assumed that early microcrack propagation is proportional to the growth of the TGO scale at the interface between TBC and bondcoat. Afterwards, up from a crack length which is determined by the roughness of the bondcoat, microcracks coalesce to macrocracks which further propagate due to

stresses induced by thermal misfits and lateral TGO growth. Spallation of the TBC occurs as soon as a defined crack length is reached [7].

a) Incubation phase.

During the incubation phase crack length is assumed to increase proportionally to the TGO thickness d_{TGO} until a TGO thickness of ¼ of the averaged peak-to-peak roughness of the BC R_Z^{BC}. is reached. The crack length *a* is calculated by:

$$a = \frac{1}{2}\lambda_R^{(BC)} \cdot \frac{4 \cdot d_{TGO}}{R_Z^{(BC)}} \quad \text{for} \quad d_{TGO} \le \frac{1}{4} R_Z^{(BC)} \tag{1}$$

λ_R^{BC} is the wavelength of the BC roughness profile.

The TGO thickness evolution is calculated using a parabolic law which was adjusted to the experimentally determined oxidation kinetics:

$$d_{TGO} = k_p (t_{T_{\max}})^n \tag{2}$$

with k_p = oxidation rate constant, $t_{T_{\max}}$ = exposure time at maximum temperature, n = oxidation exponent. The temperature dependence of k_p was assumed to follow an Arrhenius law.

Calculation of TGO growth was performed using 100 equal time increments per cycle. For each time increment an average temperature was determined. Further details about this incremental calculation method are given in [7].

b) Propagation phase.

The first part of the crack energy G_{El} is induced by thermal misfits which result in compressive in-plane- and tensile out-of-plane stresses in the TBC above the roughness profile of the BC and lead to mode I opening of delamination cracks during the cooling phase of each thermal cycle. This part of the energy release rate is calculated assuming homogenous temperature across the complete TBC system:

$$G_{el} = \frac{E_{TBC}(1-\nu_{TBC}^2)}{2(1-\nu_{TBC})^2}\left[(\alpha_{th}^{(TBC)} - \alpha_{th}^{(Sub)})(DBTT - T_{\min})\right]^2 \cdot d_{TBC} \cdot Y^2 \cdot f(r) \tag{3}$$

$\alpha_{th}^{(TBC)}$ and α_{th}^{Sub} are the thermal expansion coefficients of the TBC and the substrate alloy, respectively. DBTT is the ductile - brittle transition temperature of the bondcoat, Y the geometry factor of the crack and f(r) a correction function account for the local curvature of the substrate, e. g. at the leading edge of a turbine blade.

The second part of the energy release rate is induced by in-plane stresses due to lateral growth of the TGO which also result in compressive in-plane and tensile out-of-plane stresses above roughness peaks causing mode I opening of delamination cracks. This part of G, noted as G_{TGO}, is calculated by:

$$G_{TGO} = \frac{E_{TGO}(1-\nu_{TGO}^2)}{10(1-\nu_{TGO})^2} \cdot (\beta \cdot (1+f_{ox}))^2 \cdot d_{TGO} \cdot Y^2 \cdot f(r) \tag{4}$$

With E_{TGO} = Youngs modulus of the TGO, β = volume change during TGO growth according to the Pilling – Bedworth ratio, f_{ox} = portion of lateral growth of the TGO and f(r) = const. = 1.

With both parts of the energy release rate according to eq. (6) and (7) the crack propagation rate da/dt is calculated:

$$\frac{da}{dt} = A \cdot (G_{el} + \frac{1}{b} \cdot G_{TGO})^m \tag{5}$$

With d_{TBC} and d_{TGO} = thickness of the TBC and the TGO, respectively, A = crack growth coefficient, m = crack growth exponent and B = weighting factor for the influence of TGO growth on delamination crack propagation.

Eq. (5) is numerically integrated cycle by cycle. The end of the crack propagation phase and therewith the lifetime of the TBC is defined at the number of cycles N_f at which a critical crack length of l_{crit} = 5 mm is reached.

3.2.2 Parameter identification and model validation

Most of the model parameters are directly obtained from measurements of TGO growth during isothermal oxidation tests, stiffness measurements and dilatometry at free standing TBCs and substrate samples and by microscopic evaluation of the roughness profile at the TBC / bondcoat interface. Only three different thermal cycling experiments are used to fit the remaining parameters of the model, i.e. A, B and m in eq. (5). More detailed information about parameter identification is given in [7].

In Fig. 5a the data points from thermal cycling experiments used for parameter fitting (2 h dwell time, 60°C-1050°C; 2 h dwell time, 350°C-1050°C and 20 min dwell time, 60°C-1050°C) are marked by a rectangle. With the other results in Fig.5a and b the model was validated for in the temperature ranges 60-1050°C and 60-1100°C. It can be seen from Fig. 5 that the predictions for both temperature ranges are in good agreement with experimental data. It should also be emphasized that the range of considered high temperature dwell times covers more than four orders of magnitude.

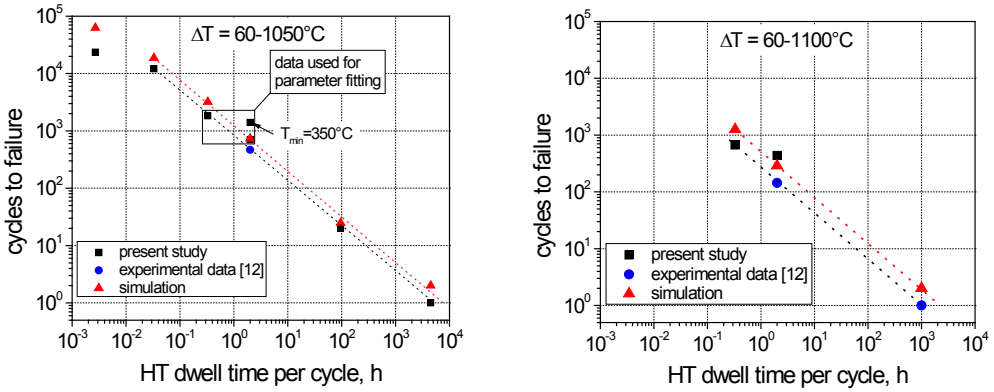

Fig. 5. Experimentally determined and predicted TBC lifetimes for thermal cycling with different HT dwell times in temperature range (a) 60-1050°C and (b) 60-1100°C.

4 Conclusions

The effects of high temperature dwell time as well as of minimum and maxim cycle temperatures on APS TBCs performance under thermal cycling were investigated. Increasing dwell time at maximum temperature leads to a decrease of the number of cycles to failure, whereas accumulated time at maximum temperature increases. An increase in minimum temperature resulted in pronounced increase of lifetime. At T_{min} = 700°C the accumulated time at maximum temperature until failure reached a similar value as for isothermal exposure. An increase in maximum temperature led to decreasing lifetime. Both, an increase of dwell time at maximum temperature and an increase of minimum temperature resulted in a shift of the failure crack path towards the TGO.

Fatigue crack growth under TMF loading is controlled by oxidation as well as by fatigue related processes. For TMF tests with short exposure at high temperature fatigue failure of the base material occurred. The application of a high temperature dwell time (2 hours at 1050°C) in the TMF cycle led to delamination failure of the TBC before fatigue failure of base material.

A model for life prediction of APS TBC under thermal cycling based on a two step approach for crack length calculation is proposed. Only three thermal cycling tests were used to fit the model parameters. The validation of the model with results from thermal cycling in different temperature ranges without additional parameter fitting revealed a good accuracy of predicted lifetimes. Considering the influence of thermal gradients across the TBC and/or mechanical strains is the subject of future research.

References

1. R.A. Miller, J. Therm. Spray Technol. **6**, 35 (1997)
2. N.P. Padture, M.Gell, E.H.Jordan, Science, **296**, 280 (2002)
3. Y.H.Zhang, P.J.Withers, M.D.Fox, D.M.Knowles, Mat. Sci. and Tech., **15**, 1031 (1999)
4. B.Baufeld, Scripta Materialia, **45**, 859 (2001)
5. E.Tzimas, Acta mater., **48**, 4699 (2000)
6. B. Heinecke, A. Scholz, C. Berger, *TurboMat* (2002)
7. T. Beck, O. Trunova, R. Herzog, R.W Steinbrech, L. Singheiser, Surface and Coatings Technology, **202** 5901 (2008)
8. O. Trunova, P. Bebnarz, R. Herzog, T. Beck, L. Singheiser, Int. J. Materials Research, **10**, 1129 (2008)
9. T. Beck, P. Hähner, H.-J. Kühn, C. Rae, E.E. Affeldt, H. Anderson, A. Köster, M. Marchionni, Materials and Corrosion, **57**, 53 (2006)
10. O. Trunova, T. Beck, R. Herzog, R.W Steinbrech, L. Singheiser, Surface and Coating Technology, **202**, 5027 (2008)
11. O. Trunova, T. Beck, R.W Steinbrech, R. Herzog, L. Singheiser, *Proc. TSM 137th Annual Meeting&Exhibition* (2008)
12. R. Herzog, P. Bednarz, O. Trunova, R.W. Steinbrech, E. Wessel, W.J. Quadakkers, F. Schubert, L. Singheiser *Proc. 8th Liège Conference on Materials for Advanced Power Engineering* (2006)